INTRAVENOUS TREATMENT WITH ISOTOPICALLY MODIFIED ^{64}ZN-ASPARTATE ALLEVIATES NEUROINFLAMMATION AND MOTOR DYSFUNCTION IN RATS WITH LPS-INDUCED PARKINSON'S DISEASE

Mariia Rudyk[1]*, Max Temnik[2], Alexandr Balakin[2], Sergey Gurin[2], Taisa Dovbynchuk[1], Roman Byshovets[3], Nataliia Dzubenko[4], Ganna Tolstanova[4], Larysa Skivka[1]

[1] Educational and Scientific Centre "Institute of Biology and Medicine", Taras Shevchenko Na-tional University of Kyiv, 2, Hlushkova Avenue, Kyiv 03022, Ukraine

[2] Physical Chemistry, Vector Vitale, North Miami Beach, USA;

[3] Department of Internal Diseases, Bogomolets National Medical University, 13, Shevchenko Blvd., Kyiv 01004, Ukraine

[4] Educational and Scientific Institute of High Technologies, Taras Shevchenko University of Kyiv, 4g, Hlushkova Avenue, Kyiv 03022, Ukraine.

* Corresponding author: Mariia Rudyk

ABSTRACT

.....

INTRODUCTION

Parkinson's disease (PD) is the second most commonly reported neurodegenerative disease after Alzheimer's disease. Currently, more than 10 million people worldwide are living with PD diagnosis, ~ 90% of cases are considered sporadic. According to WHO statistics, the prevalence of PD has already doubled in the last 25 years, and the number of people with this pathology is expected to further double by 2040 in rapidly ageing societies (Willis et al., 2022; Safiri et al., 2023). Sporadic PD is a multifactorial neurologic disorder whose etiology and pathogenetic mechanisms remain unclear. Main pathological PD hallmark - movement disorder - is a result of the loss of dopaminergic neurons (DN) in the *substantia nigra pars compacta* (number of other brain regions are also involved in the pathological process). Key histopathological feature of PD are α-synuclein-containing Lewy bodies, which are commonly registered in areas of severe neuronal loss and is a result of α-synuclein misfolding and aggregation into neurotoxic clumps. Oxidative stress associated with mitochondrial complex I dysfunction (Chen et al., 2019) and proteolytic stress due to dysfunction of the ubiquitin–proteasome system's autophagy pathway (Adam et al., 2023) are also considered as important pathogenetic mechanisms of PD. Despite considerable efforts, PD remains an incurable disease, which

treatment is limited to symptomatic therapy in large part due to the complex and not thoroughly investigated pathophysiology and heterogeneity of the disease (Alfaidi et al., 2024; Niu et al.,2025; Berg et al., 2020). More recently, chronic inflammation, both at the peripheral and cerebral levels, is considered an inevitable component of the pathological scenario in PD (Lee et al., 2019; Forloni et al., 2021). Aggregated α-synuclein initiate pro-inflammatory shift of resting microglia/macrophages. Subsequent generation of inflammatory mediators contributes to progressive neurodegeneration (Troncoso-Escudero et al., 2018). It is noteworthy that inflammation accompanies all stages of the disease and thus is a promising disease-modifying target over the entire disease course. Numerous preparations with the potential to reduce neuroinflammation (non-steroidal anti-inflammatory drugs (NSAID), microRNAs, leukotriene modifiers, Peroxisome Proliferator-Activated Receptor Gamma (PPAR-γ) agonists and many others) are widely examined in either animal/cell culture models of PD and in clinical trials (Song et al., 2024; Çınar et al., 2022). Some of them, e.g. Sargramostim - recombinant granulocyte– macrophage colony-stimulating factor - aimed at inflammation resolution by increase of regulatory T cell number and function, but has a limited therapeutic efficacy, probably due to the limited range of targets (Olson et al., 2023). Most of the aforementioned preparations possess immunosuppressive properties. Namely, NSAID exert neuroprotective effects and reduce risk of PD by inhibiting cyclooxygenases (Badawoud et al., 2024). Some of them are successfully used as an addition to conventional PD therapy (Khrieba et al., 2024). AZD3241 - a selective and irreversible myeloperoxidase (MPO) inhibitor - demonstrates promising results in phase 1/2 trials suppressing microglial activation. However, weak MPO-related immune responses at early-stage PD might be a limitation for the use of this immunomodulator (Fernández-Espejo et al., 2022). Inzomelid reduce α-synuclein deposition, rescues motor deficits, and impede neurodegeneration in phase 1 trial by inhibiting NLRP3 inflammasome (Pardo-Moreno et al., 2023). Azathioprine, which has positive effects on the progression of motor and non-motor symptoms in early PD patients, reduces the proliferation of B and T cells (Murakami et al., 2023). Common concern associated with anti-inflammatory drugs with immunosuppressive effects may be weakening patrolling function of immune system and increased risk of infectious comorbidities (Hommel et al., 2022).

Central event in persistent chronic neuroinflammation in PD is activation of NF-κB followed by uncontrolled production of pro-inflammatory mediators by activated microglia and astroglia, which can cause DN degeneration and apoptosis. Therefore, inhibiting NF-κB pathways may be promising approach of counteracting neuroinflammation for PD treating (Xue et al., 2024). One of the potent modulators of NF-κB

pathway is zinc whose anti-inflammatory properties are widely reported (Liu et al. 2023; Briassoulis et al., 2023). Namely, zinc induces the expression of main negative regulators of NF-κB activation - zinc-finger proteins A20 and PPAR-α (Wessels et al., 2017). However, zinc inhibits inflammation while preserving the patrolling function of the immune system by protecting cells from reactive oxygen species-mediated damage during immune activation and by preserving cell membrane integrity (Gammoh & Rink 2017). Zinc also exerts an effect on the cell redox state, alleviating oxidative stress. Namely, zinc is one of the most potent inducers of transcription and synthesis of metallothioneins - intracellular free radical scavengers, and the glutathione (a major cellular antioxidant) (Jarosz et al., 2017). In addition, zinc ions hinder α-synuclein aggregation by augmenting chaperone function of human serum albumin (Al-Harthi et al., 2022).

The clinical effects of zinc supplementation, especially in elderly persons with inflammaging are very conspicuous and have a significant impact on health (Prasad et al., 2014; Kiouri et al., 2023). Several reports describe neuroinflammation decline and cognitive improvements after zinc supplementation in animal models and clinical trials. Namely, zinc supplementation decreased neuroinflammatory parameters in obese rats after a high-fat diet (Feijó et al., 2022; Hafez et al., 2023), as well as in overweight and obese women (de Vargas et al., 2023). Zinc supplementation during pregnancy alleviates neuroinflammation in offspring on the animal model of neuropsychiatric disorders (Mousaviyan et al., 2021), as well as suppresses prenatally stress-induced behavioral and neurobiological impairments in adolescent female rat offspring (Semeei et al., 2023). In addition, zinc supplementation improves lifespan and motor capacities in a drosophila with a mutant Parkin - zinc-binding E3 ligase, whose mutation results in autosomal recessive juvenile PD in human (Saini & Schaffner 2010). In rats with rotenone-induced PD, zinc supplementation has neuroprotective effects reducing lipid peroxidation and neuronal death (Mbiydzenyuy et al. 2018). Zinc supplementation demonstrates promising results in patients with Alzheimer disease (Squitti et al., 2020).

All these studies have utilized zinc compounds with natural isotopic composition. Zinc comprises five stable isotopes: ^{64}Zn, ^{66}Zn, ^{67}Zn, ^{68}Zn, and ^{70}Zn, with average natural abundances of 48.6%, 27.9%, 4.1%, 18.8%, and 0.6%, respectively. Among these, ^{64}Zn and ^{66}Zn are the most prevalent, making the ^{66}Zn/^{64}Zn ratio, expressed as δ^{66}Zn, a standard metric for assessing zinc isotopic compositions in mammalian tissues (Jaouen et al., 2019). A key characteristic of zinc homeostasis in a healthy brain is the dominance of the lighter isotope ^{64}Zn (δ^{66}Zn < 1). This phenomenon is attributed to the distinct chemical bonding patterns of zinc in various tissues. Zinc forms tight bonds with oxygen- and nitrogen-containing groups (e.g., sulfate, phosphate, lactate,

histidine), which favor the heavier isotope, while its bonds with sulfur-containing groups (e.g., cysteine, methionine) favor the lighter isotope. In a healthy brain, most zinc is bound to cysteine residues within metallothioneins (Tanaka and Hirata, 2018; Solovyev et al., 2021). According to current hypotheses, the heavier zinc isotope accumulates progressively in the human body, leading to an increase in $\delta^{66}Zn$ with age (Albarede et al., 2016; Jaouen et al., 2019). This redistribution of zinc isotopes in the brain is particularly evident in neurological disorders linked to protein misfolding (Moynier et al., 2020). For instance, in Alzheimer's disease (AD) brains, heavy zinc isotopes preferentially bind to histidine residues within the N-terminal hydrophilic region of amyloid-β (Aβ) peptides, particularly in amyloid-β plaques. Although the specific role of metal binding in the normal biological functions, aggregation, or conformational alterations of alpha-synuclein remains insufficiently explored, it is the histidine at residue 50 (which is the binding site for heavy zinc isotope (Ramis et al., 2018) that plays crucial role in α-synuclein misfolding and aggregation into neurotoxic clumps (Brown et al., 2009; Nakamura et al., 2023).

Zinc supplements are typically administered orally, but their therapeutic effectiveness is often limited. One potential explanation is the age-related decline in intestinal zinc absorption. Parenteral supplementation offers a potential solution to this limitation (Cvijanovich, 2016; Baltaci, 2024; Gumus, 2023). To the best of our knowledge, this study represents the first investigation into the effects of intravenous (i.v.) delivery of isotopically modified zinc in an animal model of PD. This study aimed to evaluate the impact of i.v. administration of ^{64}Zn di-aspartate (KLS-1) on neuroinflammation and, as a result, on motor dysfunction in rats with LPS-induced (inflammatory) PD model.

In this study, we employed a novel zinc-aspartate (KLS-1) comprising isotopically modified zinc, where light isotope ^{64}Zn was enriched to a mass fraction of 99.2% - a significant enhancement compared to the natural isotopic ratio of 48.6% commonly used in zinc supplements discussed in the literature. Previous experiments demonstrated that KLS-1 exhibited greater biological activity compared to zinc aspartate with a natural isotopic distribution (Novak, 2022; Novak, 2022(1)).

MATERIALS AND METHODS

Test Agent. Isotopically modified ^{64}Zn di-aspartate (^{64}Zn-asp), an investigational new complex of zinc aspartate (Fig. 1), was used as a therapeutic test agent. The compound molecule consists of two molecules of

L-aspartic acid (NeoFroxx, Einhausen, Germany) and one atom of ^{64}Zn, having its molecular formula of $C_8H_{12}O_8N_2{}^{64}Zn$ (Fig.1).

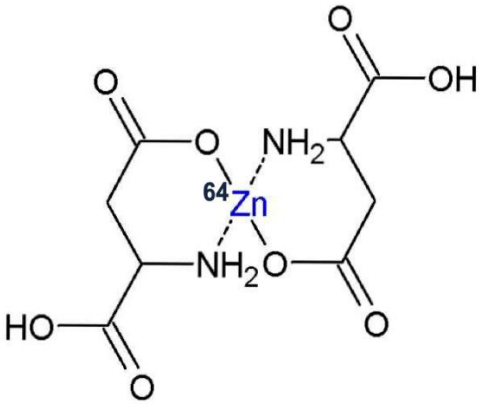

Fig. 1. Schematic representation of the investigational new compound structure.

The molar mass of the compound in solution is 328 g/mol. The proportion of zinc in the compound is 17.98%. The zinc in the compound consisted of stable light isotope ^{64}Zn enriched to 99.2% mass fraction of total zinc. KLS-1 was manufactured by Pharmaceutical Factory Biopharma LLC (Bila Tserkva, Ukraine) - forming a chelate complex (Fig.1).

Animals, Study Design and LPS-PD Model. Experiments were conducted on adult male Wistar rats (8 weeks old, 220-250 g) bred in the vivarium of the Educational and Scientific Centre "Institute of Biology and Medicine" of Taras Shevchenko National University of Kyiv, Ukraine. The animals were kept in standard conditions with ad libitum access to water and food (standard diet). Animal protocols were approved by the University Ethics Committee (protocol No 4, 10.10.2021) according to Animal Welfare Act guidelines. All procedures with animals were performed in accordance with the principles of humanity as stated in "General principles of animal experimentation" approved by the National Congress on bioethics (Kyiv, 2001–2007) and in concordance with Council directive of November 24, 1986 on the approximation of laws, regulations and administrative provisions of the Member States regarding the protection of animals used for experimental and other scientific purposes (86/609/EEC). Before the experiment, 66 adult male Wistar rats were randomly divided into 4 groups using the "RAND ()" function in Microsoft Excel (Fig.2A): group I - intact animals (n=12); group II - sham-operated animals (n=12); group III - LPS-PD (n=12); group IV – rats with LPS-PD treated with ^{64}Zn-asp (n=15). In order to attain unilateral lesions of the nigrostriatal system in animals from

group III and IV, stereotaxic microinjections of 10 µg of LPS (Lipopolysaccharide from *Escherichia coli* O111:B4, Sigma) at the volume of 2 µl of sterile physiological saline (JSC "Infusion", Ukraine) were conducted. Animals from groups II were injected with 2.0 µL of sterile physiological saline. Before the surgery, rats from groups II-IV were anesthetized with a mixture of ketamine (75 mg/kg diluted in sterile water for injection, Sigma, USA) and 2% Xylazine (400 µl/kg, Alfasan International BV, Netherlands) i.p, placed in a stereotaxic instrument (SEJ-4, Ukraine). After that, either LPS or sterile physiological saline was injected unilaterally into the brain through the drilled burr hole directly into the *substantia nigra* (AP 5.3 mm, ML ± 2.0 mm (from bregma), and DV 7.2 mm (below dura)) according to Hoban et al. (2013). The injections were performed at a rate of 1 µl/min (every 15s). The injector was left in place for 5 min before slowly withdrawing it to allow for the toxin diffusion and to prevent the toxin reflux. The period of 8 days was allowed for the development of LPS-induced model of Parkinson's disease (PD.) Animals from groups IV received 10 daily i.v. injections of ^{64}Zn-asp into the lateral tail vein at a dose of 1.5 mg/kg starting from Day 9 after the disease initiation. PD development was ascertained by the results of behavioral testing and post-mortem assessment of nigrostriatal neurodegeneration using semi-quantitative tyrosine hydroxylase (TH) immunohistochemistry. Metabolic profile of microglia/macrophage population, as well as astroglia assessment were evaluated at the time point of the experiment cessation (Day 28 after the surgery) (Fig.2B).

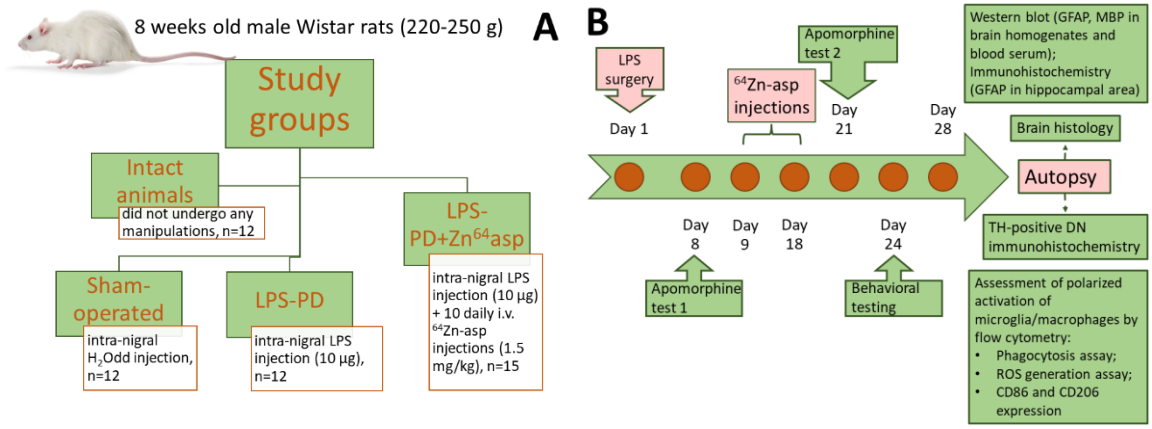

Fig. 2. Animal groups (A) and study design (B).

Behavioral Testing. Open field test was conducted on Day 24 after the surgery as described by Leite-Almeida et al., 2009). To evaluate voluntary movement, anxiety, and exploratory behavior in new environment, the rats were tested in the Open Field arena conformed of a square field with sides of 100 cm and a wall height

of 30 cm, which illuminated by two LED lamps (each with 60W) placed at a height of 2 m) for 5 minutes. A grid of 36 squares was drawn on the bottom of the arena. During testing, each animal was individually placed in the center of the arena and its ambulatory activity was recorded using a digital camera ("Casio® EX-Z850", China, which was located above the center of the arena at a height of 1 m) followed by the analysis using MATLAB. The following behavioral characteristics were assessed: total distance travelled, time spent exploring the inner perimeter, time spent in squares surrounded by two walls (thigmotaxis), number of rearing and grooming, frequency of defecations (Sestakova N et al., 2013; Lamprea et al., 2008). The arena was cleansed and allowed to dry after each animal test.

Apomorphine test was conducted on Day 8 and Day 21 after the surgery. Apomorphine (Sigma, USA) was i.p. administered to the lesioned rats at a dose of 0.5 mg/kg. Five minutes after the injection, the rats were put individually into a 40 cm-diameter cylinder and the counterclockwise (contralateral) rotations were monitored and registered for 30 min using a stopwatch (Smith et al., 2012). Animals scoring over 6 rpm were considered as lesioned with 86.6% DN loss. Rats scoring less than 6 rpm (0-2 rpm) were considered as lesioned with 44% DN loss (Talanov et al., 2006).

Elevated plus maze (EPM) test was used to assess anxiety-like animal behavior and was conducted on Day 24 after the surgery (Walf and Frye, 2007). EPM raised to a height of 50 cm from the floor was consisted of cross-shaped field with two opposite open arms (50 cm x 10 cm) and two closed arms (50 cm x 10 cm x 30 cm). These four arms were connected to a center square with sides 10 cm into which, facing the open sleeve, the animal is placed at the beginning of the test. The setup was illuminated by two LED lamps, each 60 W, which are located at a height of 2 m. The experiment is recorded on an IP camera, after which the parameters are evaluated using MATLAB. Behavioral assessment was performed using following main parameters: total distance traveled, number of transitions from open to closed arms, number of transitions from closed to open arms, time spent in open and closed arms, total number of transitions and time spent in a stretched attend posture (risk assessment) (Walf and Frye, 2007). The testing was conducted for five minutes. Before starting the measurements, animals underwent an adaptation period to the new environment in order to reduce their stress state.

Histological Examination of the Rat Brains. A procedure of rapid, controlled and uniform fixation of the entire body of the animal was carried out under light ether anesthesia using 4% buffered paraformaldehyde

(Diapath, Italy) perfused through the rat's heart (Gage et al., 2012). The brain was carefully removed and fixed in 10% neutral formalin (Diapath, Italy). Fixed frontal tissues were dehydrated and embedded in Paraplast (Surgipath Paraplast, Leica, USA). 6-μm thick paraffin sections of the brain were cut using a Thermo Microm HM 360 microtome (Thermo Scientific, USA). Sequentially, the sections were deparaffinized, rehydrated and stained with hematoxylin and eosin (Thermo Scientific, USA) using standard procedures (Falkeholm et al., 2001; Buesa and Peshkov, 2011). Topography of the *substantia nigra* of the rat midbrain was determined using a stereotaxic atlas (Paxinos and Watson, 1982). The presence of a microinjector track served as a criterion for localization of the damage zone in brain samples from rats of experimental groups (groups II-IV). The stained slides were examined using an Olympus BX51 microscope (Olympus, USA). Microphotographs of homotopic areas of the *substantia nigra* were obtained and morphometric analysis of changes in the average cross-sectional areas of neuron bodies (perikaryons) was performed using AxioVision SE64 Rel.4.9.1 software (Carl Zeiss, Germany) at a magnification of ×400.

Immunohistochemistry. For immunohistochemical staining of rat brain sections with antibodies to tyrosine hydroxylase (TH), rats were deeply anesthetized and transcardially perfused with heparinized (5000 U/L) sterile physiological saline (100 ml) followed by 4% paraformaldehyde (150 mL, pH 7.4). The brains were removed, post-fixed in 4% paraformaldehyde, and sectioned. The paraffin-embedded sections (5 μm) were processed for TH immunohistochemical detection using ABC–peroxidase method as described previously (Walsh et al., 2011). Briefly, tissue sections were first incubated with tyrosine hydroxylase (TH) primary antibodies (1:200, Millipore, AB152, USA) overnight (4 ºC), and then with the secondary anti-rabbit biotinylated antibodies (1:200) for 60 min. After this, Diaminobenzidine (Dako, EnVision Flex, DM821, USA) immunoreactivity detection system was applied for 5 min. Stained sections were assessed using a Primo Star microscope (Carl Zeiss, Germany). Each sample was scored semi-quantitatively as to the intensity of immunostaining on a four-point scale, with 0 indicating absence of staining (<10% of positive cells), 1+ indicating the lowest level of detectable staining (10-25% of positive cells), 2+ indicating moderate homogeneous staining (25-50% of positive cells), 3+ indicating intense homogeneous staining (50-75% of positive cells), and 4+ (>75% of positive cells) (Pauletti et al., 2000). The results were scored by multiplying the percentage of positive cells (P) by the intensity (I) and presented as Quick score (Q): Q = P x I.

Hippocampal sections were prepared to detect GFAP expression in the rat brain tissue using confocal microscopy. The sections were blocked with 3% bovine serum albumin (Sigma-Aldrich, Germany) for 60 minutes at room temperature. The tissue sections were incubated with primary anti-GFAP antibodies (Santa Cruz Biotechnology, USA) at +4˚C overnight. Sequentially, the samples were incubated for 60 min at room temperature with FITC-conjugated secondary antibodies (Santa Cruz Biotechnology, USA) diluted 1:500. The slides were rinsed and stained with fluorescent dye Hoechst-33342 (Invitrogen, United Kingdom) to visualize the cell nucleus. Immunofluorescence results were analyzed using an LSM 510 META microscope (Carl Zeiss, Germany) and processed using ImageJ software (Fiji, USA).

Western Blot Analysis. To isolate proteins, freshly isolated rat brain samples were rapidly placed in liquid nitrogen and crushed. Sequentially, the brain tissues were lysed and proteins were extracted using RIPA buffer (Sigma-Aldrich, USA). All lysates were subsequently sonicated three times for 30 s (Sartorius, Labsonic® M, Canada) and centrifuged at 16000g for 30 min at +4°C (Sigma-Aldrich, USA). The protein concentrations in rat brain samples were measured using the Modified Lowry Protein Assay Kit (Thermo Scientific, USA) following the manufacturer's instructions. Supernatants were diluted with 5× Laemmli sample buffer (Sigma-Aldrich, USA) containing 0.1 M dithiothreitol (Sigma, USA) and boiled for 5 min. Protein samples were subsequently frozen and stored at -20°C. Protein electrophoresis was performed in Tris-glycine buffer (pH 8.3) (Sigma-Aldrich, USA) using a Mini-PROTEAN II electrophoresis chamber (BIO-RAD, USA) at a voltage of 100 V for 90 min. To determine molecular weights of proteins on electropherograms, protein standards covering a molecular weight range of 10-250 kDa (Thermo Scientific, USA) were used. Proteins were transferred from polyacrylamide gel (Sigma-Aldrich, USA) onto a 0.45-µm pore size nitrocellulose membrane (RPN 203D, GE Healthcare, Amersham Bioscience) using the Mini Trans-Blot Cell (BIO-RAD, USA) in a transfer buffer containing 2.5 mmol/L Tris-HCl, pH 8.3, 20% methanol, 192 mmol/L glycine, 0.1% SDS (Sigma-Aldrich, USA). Free binding sites on the membrane were blocked with 5% skim milk (Genesee Scientific Inc., USA). The membrane was incubated with primary anti-GFAP antibodies (Santa Cruz Biotechnology, USA), myelin basic protein (MBP) (Santa Cruz Biotechnology, USA) or beta-actin (Santa Cruz Biotechnology, USA) diluted in phosphate buffer saline containing 0.05% Triton X-100 (Sigma-Aldrich, USA) following the manufacturer’s instructions at +4˚C overnight. Sequentially, the membrane was incubated with horseradish peroxidase-conjugated secondary antibodies (Santa Cruz Biotechnology, USA) for 60 minutes.

Immunoreactive bands were visualized using enhanced chemiluminescence. Densitometric analysis of autoradiograms was performed using TotalLab TL120 software (Nonlinear Inc., USA) and the intensity of bands was normalized to the intensities of corresponding beta-actin bands. The protein number was reported in arbitrary units (a.u.).

Microglia/Macrophage Cell Isolation. For microglia/macrophage cells isolation, brain was rapidly extracted on ice. Hippocampus was dissected and perfused using a phosphate buffered saline (PBS). Isolated tissue was softly dissociated in ice cold PBS supplemented with 0.2 % glucose for 15 min at room temperature using Potter homogenizer. Tissue homogenate was filtered through a 40 nm cell strainer (BD Biosciences Discovery) for additional tissue grinding and subsequently carried to a 15 mL tube and centrifuged at 350 g for 10 minutes at room temperature. Cell sediment was suspended in 1 ml of 70 % isotonic Percoll solution. 1 ml of 50 % Percoll solution was gently layered on top of the 70 % layer, and 1 ml of PBS solution was subsequently layered on top of the 50 % Percoll layer. Density gradient was centrifuged for 40 min at 1200 g. After centrifugation, the layer at the interface between the 70 % and 50 % Percoll phases contained highly enriched microglia/macrophage was aspirated and cells were washed twice in PBS by centrifugation (Frank et al., 2006). Purity of isolated microglia/macrophage fraction was examined by flow cytometry using fluorescein isothiocyanate (FITC) mouse anti-rat CD11b (BD PharmingenTM) and phycoerythrin (PE) mouse anti-rat CD45 (BD PharmingenTM). The proportion of CD11b+CD45+ cells was 88.9 ± 3.7 %. Cell viability was determined by Trypan blue exclusion test. The proportion of viable cells was ≥ 93 %.

Phagocyte Metabolic Profile Assessment. A phagocyte metabolic profile was characterized by their phagocytic activity, oxidative metabolism, and phenotypic marker expression, which were examined by flow cytometry. Phagocytic activity was detected as described earlier (Rudyk et al., 2018). FITC-labeled thermally inactivated cells of *Staphylococcus aureus* Cowan I (collection of the Department of Microbiology and Immunology, ESC "Institute of Biology and Medicine" of Taras Shevchenko National University of Kyiv) were used as a phagocytosis object. $2x10^5$ microglia/macrophage cells were incubated at 37°C for 30 min with bacterial cells (5 μL of the stock suspension of FITC–labeled *S. aureus* at a concentration of $1×10^7$ cells/mL). Phagocytosis was stopped by adding a 'stop' solution (PBS with 0.02% EDTA and 0.04% paraformaldehyde). The data was presented as the phagocytosis index (PhI) representing the mean fluorescence per one phagocytic

cell (ingested bacteria by one cell), and as phagocytosis percentage (PP) (percentage of cells emitting fluorescence). The phagocyte oxidative metabolism was examined using 2'7'-dichlorodihydrofluorescein diacetate (H2DCFDA, Invitrogen) as described previously (Rudyk et al., 2018).

For phagocyte phenotyping, FITC-labeled anti-CD86, PE-labeled anti-CD80, and Alexa Fluor 647-labeled anti-CD206 antibodies (BD Pharmingen, USA) were used. Results were assessed using FACSCalibur flow cytometer and CellQuest software (BD, USA).

Statistical Analysis. Statistical analysis was conducted using the Statistica 12.0 package. First, the data was tested for normal distribution using the Shapiro-Wilk test (Mishra et al., 2019). Normally distributed variables were presented as mean ± SD. Non-normally distributed variables were presented as the median and interquartile range (IQR). Statistical differences were calculated using ANOVA with Tukey's post-hoc test for multiple comparisons of variables with a normal distribution, and non-parametric Mann-Whitney U test for single comparisons, and Kruskal-Wallis's test for multiple comparisons of variables with a non-normal distribution (Chan and Walmsley, 1997). Differences were considered significant at $p \leq 0.05$.

RESULTS

Treatment with ^{64}Zn-asp Mitigated Reactive Astrogliosis in Rats with LPS-PD. Reactive astrogliosis is a common pathological hallmark of neurodegeneration and key component of neuroinflammation (Kwon et al., 2020). Reactive astrogliosis is accompanied by enhanced fibrillogenesis due to increased expression of glial fibrillary acidic protein (GFAP), the main intermediate filament protein component of the astrocyte cytoskeleton (Liddelow et al., 2017). Soluble GFAP breakdown products, which are released into interstitial fluid and are also found in serum, indicate neuroinflammation and neurodegeneration (Yamashita et al., 2023). In our experiments, GFAP levels in brain homogenates of LPS-lesioned rats were ~ 2 times higher as compared to the rats from control groups (Fig.3 A, B). Results of Western-blot analysis were confirmed by immunohistochemistry assay of hippocampal sections. Strongly increased immunoreactivity for GFAP was observed in LPS-lesioned rats (Fig.3D). Treatment with ^{64}Zn-asp was associated with a decrease of GFAP-immunoreactive areas in hippocamps of the rats with LPS-PD.

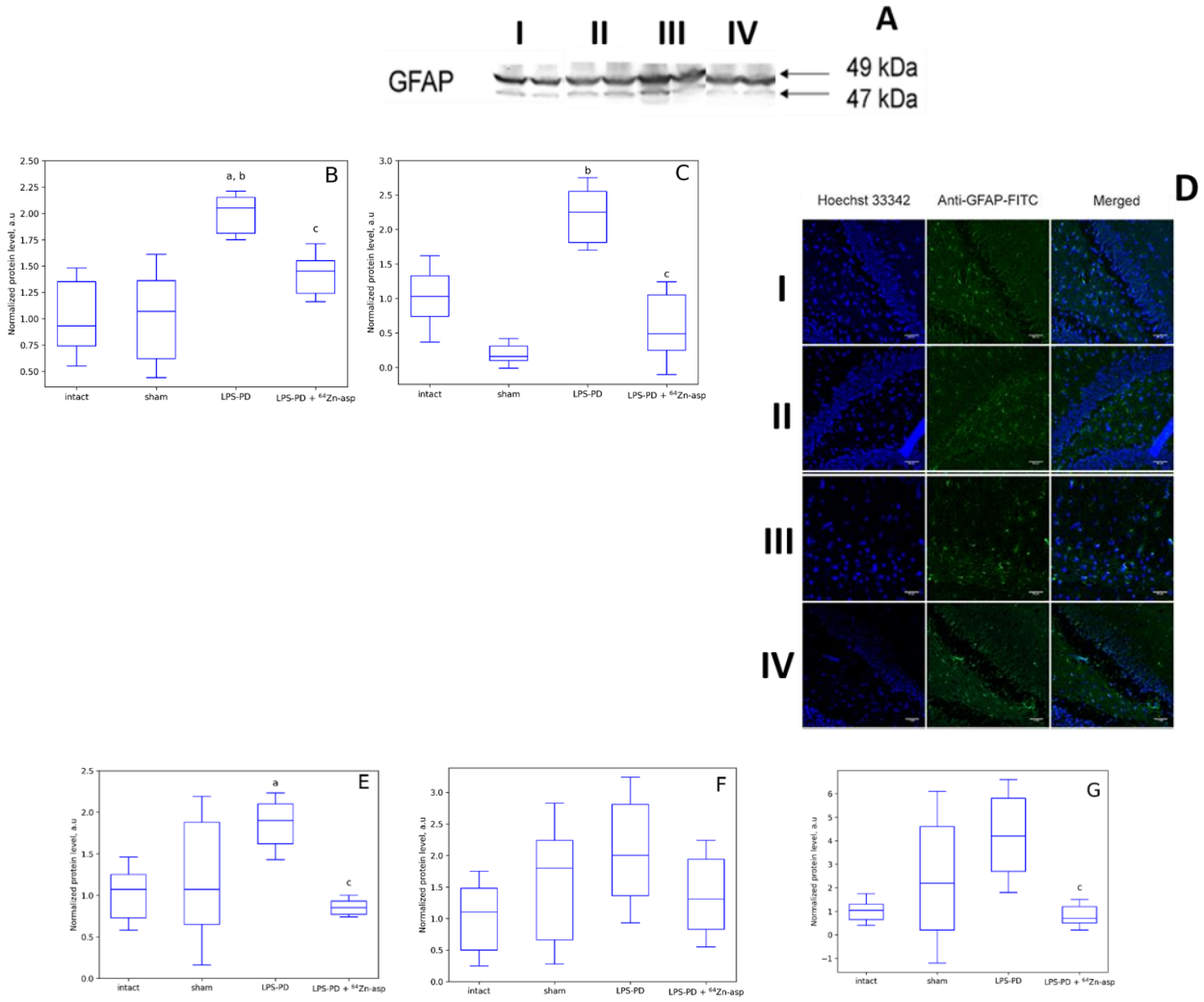

Fig.3. Effect of treatment with ^{64}Zn-asp on astroglia in LPS-lesioned rats. Western blot analysis (A) and results of blotogram densitometry of total GFAP pool (B), GFAP breakdown products (C), and MBP (E) in rat brain homogenates. D - representative immunohistochemical images of the GFAP-positive neurons in hippocampal area: I - intact animals, II - sham-operated animals, III - LPS-PD, IV - LPS-PD + ^{64}Zn-asp. Sections were treated with antibodies against GFAP and nuclei were stained with Hoechst-33342, confocal microscopy (scale bar - 50 μm). Western blot analysis of total GFAP pool (F) and GFAP breakdown products (G) in rat blood serum. Numerical data are presented as medians and IQR. a - $p \leq 0.05$ as compared to intact animals, b - $p \leq 0.05$ as compared to sham-operated animals; c - $p \leq 0.05$ as compared to LPS-PD group (Kruskal-Wallis's test).

The content of GFAP breakdown products in brain homogenates of rats from LPS-PD group was about 2.5 times higher than those in intact animals, and more than 6 times higher as compared to sham-operated rats

(Fig.3C). Slightly elevated content of GFAP and its breakdown products were also registered in serum, further indicating reactive astrogliosis in LPS-PD rats (Fig.3 F, G).

After treatment with ^{64}Zn-asp (LPS-PD+^{64}Zn-asp group), the content of GFAP and its breakdown products in animal brain homogenates decreased almost to the level of control animals. ^{64}Zn-asp injections in LPS-lesioned rats resulted also in significant decrease of serum levels of GFAP and its breakdown products additionally indicating reactive astrogliosis mitigate.

Reactive astrocytes can negatively affect myelination/remyelination and even can cause demyelination (Nash et al., 2011). In our experiments, we used Western blot for assessing MBP content in rat brain homogenates. The rat brain MBP is represented by two forms: high molecular weight polypeptides (95-110 kDa), which are components of Schwann cell membranes, and a monomeric relatively low molecular weight form (17 kDa), which is predominantly cytosolic. Assessing MBP content and its polypeptide composition in brain tissue is used to characterize the degree of neuron demyelination/remyelination (Weil et al., 2016). In our experiments, the level of high molecular weight MBP polypeptides (95-110 kDa) in the brain homogenates of animals with LPS-PD was 1.8 times higher as compared to control animals (Fig.3E). In rats with LPS-PD given the ^{64}Zn-asp injections, a decrease in the level of MBP was observed almost to the control values.

Treatment with ^{64}Zn-asp Shifted Metabolic Profile of Microglia/Macrophage Population in Rats with LPS-PD. In our experiments, complex population of microglial (MG) cells were examined. In healthy brain of intact animals, yolk sac-derived resident microglial cells predominate with minor fraction of border-associated macrophages (BAM), whereas in lesioned animals, macrophage fraction is larger due to blood monocytes recruited in the course of neuroinflammation (Silvin et al., 2023). Since counteracting NF-κB signaling is one of the key mechanisms of zinc anti-inflammatory effects, in our experiments, metabolic profile of complex MG population was characterized by assessing principal NF-κB-dependent phagocyte functions: phagocytic activity, ROS generation, and expression of phenotypic markers CD86 and CD206. Phagocytic activity was assessed using bacterial cells as phagocytosis object. Bacterial phagocytosis is toll-like receptor (TLR)-dependent process, and *S. aureus* phagocytosis involves NF-κB activation (Zhu et al., 2014). Intracellular ROS generation involves transcription of NF-κB-dependent genes, although the levels of NF-κB activity are also regulated by the levels of ROS generation. Antigen presenting capacity (including MHC- and co-stimulatory molecules CD80/86 expression) is dependent on NF-κB activation (Mussbacher et al., 2023). NF-κB also

governs mannose receptor functioning, and NF-κB inhibitors reduce the CD206 expression (Cornice et al., 2024). In our experiments, different patterns of MG metabolic state were observed in different animal groups. Metabolic characteristics of MG population in sham-operated animals indicated activated state of these cells with slight skew to M2b (anti-inflammatory, immunoregulatory) phenotype: increased fraction of phagocytizing cells and elevated phagocytic activity (Fig.4A, B), augmented ROS generation (Fig.4C), but decreased CD206+ cell fraction (Fig.4E) (Kisucká et al., 2021; Wang J. et al., 2023) as compared to intact animals. This may be due to the resolution of neuroinflammation, which is characteristic after surgical trauma during the placebo surgery (Alam et al., 2018). Values of PP, PI (Fig.4A, B) and ROS generation (Fig.4C) in MG of rats from LPS-PD group did not differ significantly from those in intact animals and were lower than those in sham-operated rats. CD86+ cell fraction in these animals was slightly smaller than that in sham group and somewhat enlarged as compared to that in intact rats (Fig.4C). CD206+ cell fraction in LPS-PD animals did not differ from that in intact rats and was higher than in animals from sham group (Fig.4E). Given the presence of neuroinflammation, which was evidenced by reactive astrogliosis, functional profile of MG in LPS-PD rats can be characterized as metabolic exhaustion with a residual level of pro-inflammatory polarized activation (Pérez & Rius-Pérez 2022; Yunna et al., 2020). Treatment of LPS-lesioned rats with 64Zn-asp significantly increased the phagocytic activity of microglia, slightly reduced the CD86+ cell fraction, and markedly decreased the proportion of CD206+ cells.

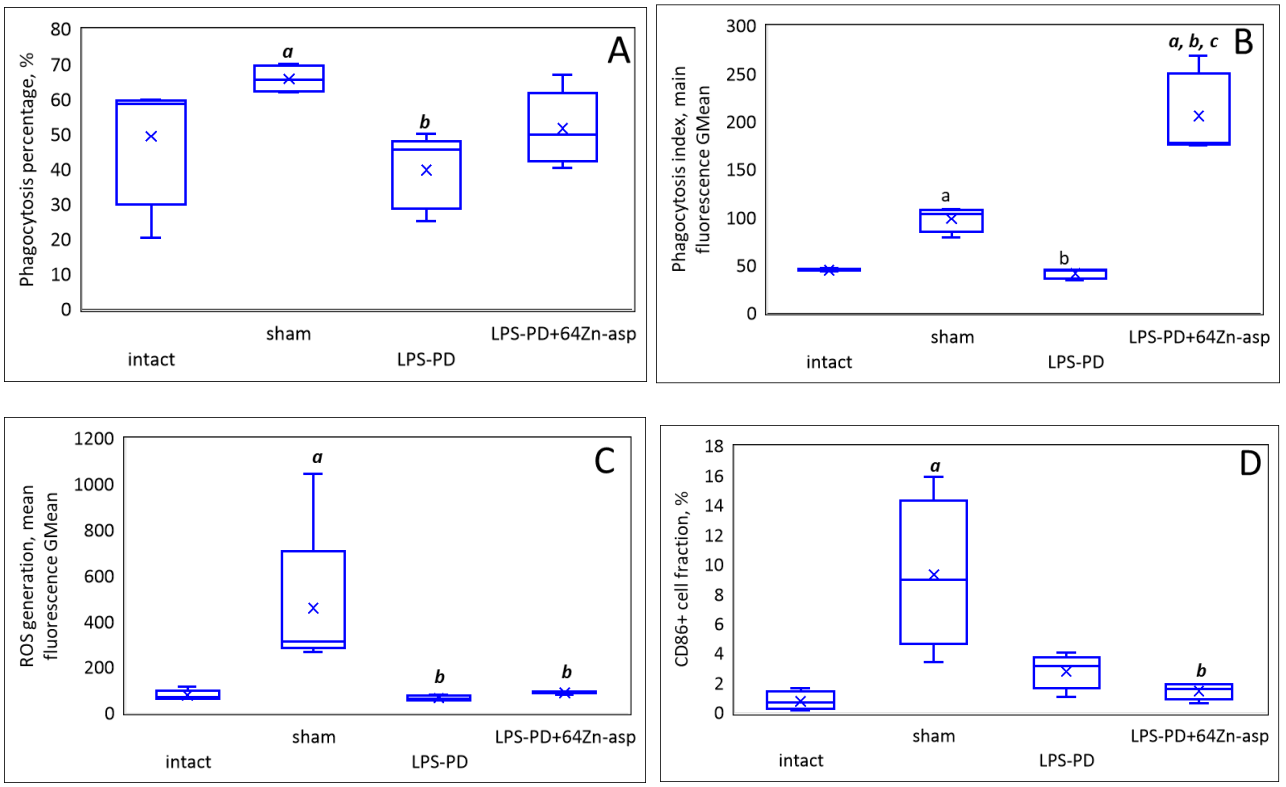

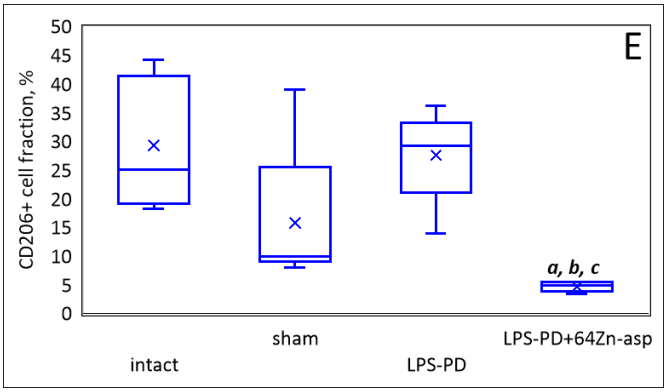

Fig.4. Effect of treatment with ^{64}Zn-asp on metabolic characteristics of microglia/macrophages in LPS-lesioned rats. A – phagocytosis percentage; B – phagocytosis index; C – ROS generation; D – fraction of CD86-positive cells; E – fraction of CD206-positive cells. Data are presented as medians and IQR. a - $p \leq 0.05$ as compared to intact animals, b - $p \leq 0.05$ as compared to sham-operated animals; c - $p \leq 0.05$ as compared to LPS-PD group (Kruskal-Wallis's test).

The fact, that PI median values in the LPS-lesioned rats treated with ^{64}Zn-asp were the highest and had surpassed similar indicators in the intact animals, the sham-operated and the LPS-lesioned untreated animals by 3.9, 1.7 and 4 times correspondingly indicates potent stimulatory effects of ^{64}Zn-asp on the phagocytic (scavenging) capacity of microglia/macrophage cells, that is characteristic for the M2a (tissue healing, neuroprotective) MG phenotype (Wang J. et al., 2023).

Treatment with ^{64}Zn-asp Prevented Body Weight Loss in LPS-lesioned Rats. Body weight loss is typical for patients with PD. This can be caused by decreased food intake, elevated energy expenditure or gastrointestinal dysfunction, and is associated with poor prognosis (Cumming et al., 2017). At the time of experiment cessation (Day 28), weight of intact animals increased by 36% as compared to initial values (Fig. 5A). Sham-operated rats gained their weight by 30,6% over this time period, whereas body weight of LPS-lesioned animals did not change for the whole of the study's observation time. LPS-lesioned rats, which received ^{64}Zn-asp injections, demonstrated slight increase in weight (by 12%) at this time point. It is necessary to note that initial body weight values in LPS-PD and LPS-PD+^{64}Zn-asp did not differ significantly (Fig.5B).

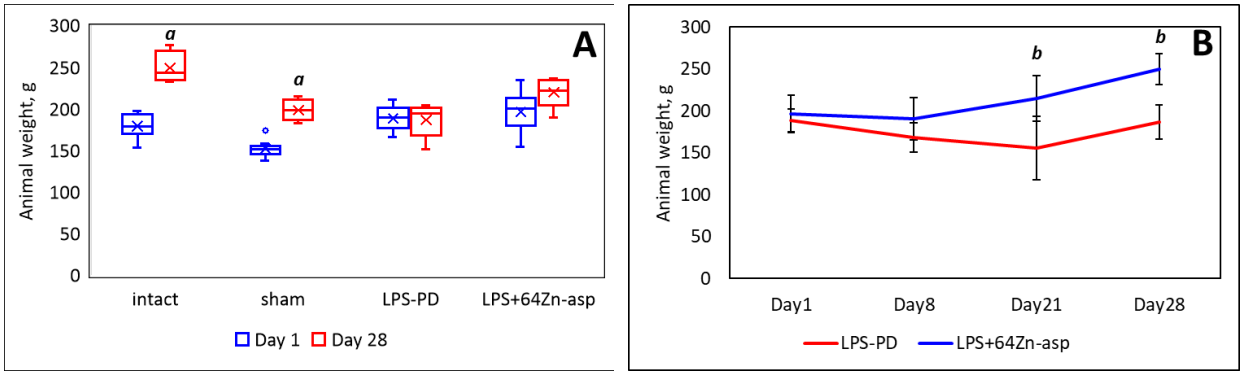

Fig.5. Effect of treatment with ^{64}Zn-asp on body weight in LPS-lesioned rats. A - changes in weight in all groups of animals at the time of experiment cessation; B - weight variation in LPS-lesioned rats with and without treatment with ^{64}Zn-asp over the time of the observation. Data are presented as medians and IQR. a – $p \leq 0.05$ as compared to value at Day 1, b - $p \leq 0.05$ as compared to untreated LPS-lesioned rats (Mann-Whitney U test).

Slow body weight loss was registered in both these groups seven days after surgery (Day 8). During the following two weeks, the weight of the LPS-lesioned animals continued to decrease. Whereas in animals from LPS-PD+^{64}Zn-asp group, which received treatment over this time period, we observed slow weight gain. It indicates the positive effect of the preparation on this non-motor symptom of the disease.

Treatment with ^{64}Zn-asp Reduced DN Loss and Behavioral Alterations in Rats with LPS-PD. Inhibition of neuroinflammation in LPS-lesioned rats after the treatment with zinc was associated with behavioral improvements and reduced DN loss.

For assessing neuronal damage in substantia nigra, morphometric neuron analysis and immunohistochemical study of the expression level of TH, a marker of DN, were carried out. The topography of the substantia nigra was determined using a stereotactic atlas (Paxinos & Watson 1982). The criterion for determining the location of the lesion (in sham-operated and LPS-lesioned animals) was the presence of a needle track. Morphometric parameters of neurons are shown in Table 1.

Table 1

Morphometric parameters of neurons of the substantia nigra in the rat brain, Me [LQ - UQ]

Animal group	Neuronal area, μm^2

Intact animals	500.4 [371.7 – 701.6]
Sham-operated	283.5 [246.4 – 343.5]*
LPS-PD	204.0 [158.6 – 285.3]*#
LPS-PD + ^{64}Zn-asp	270.6 [215.4 – 336.4]#^

*Notes: * - p<0,05 as compared to intact animals; # - p<0,05 as compared to sham-operated animals; ^ - p<0,05 as compared to untreated LPS-lesioned rats (Kruskal-Wallis's test).*

The values of intact animals are presented as averages of the right and left anatomical structures. For sham-operated and LPS-lesioned rats, the average values of morphometric parameters of the neurons of the ipsilateral area are presented. Fig. 6 shows microphotographs of the injection area (needle track) and the area of damaged substantia nigra. In the group of intact animals, no damaged neurons were found in the study area (Fig.6A and B). In the group of sham-operated rats, we observed the following lesions: reduction in the number of neurons, glial reaction and products of cell and erythrocyte destruction (hemosiderin) (Fig.6C and D).

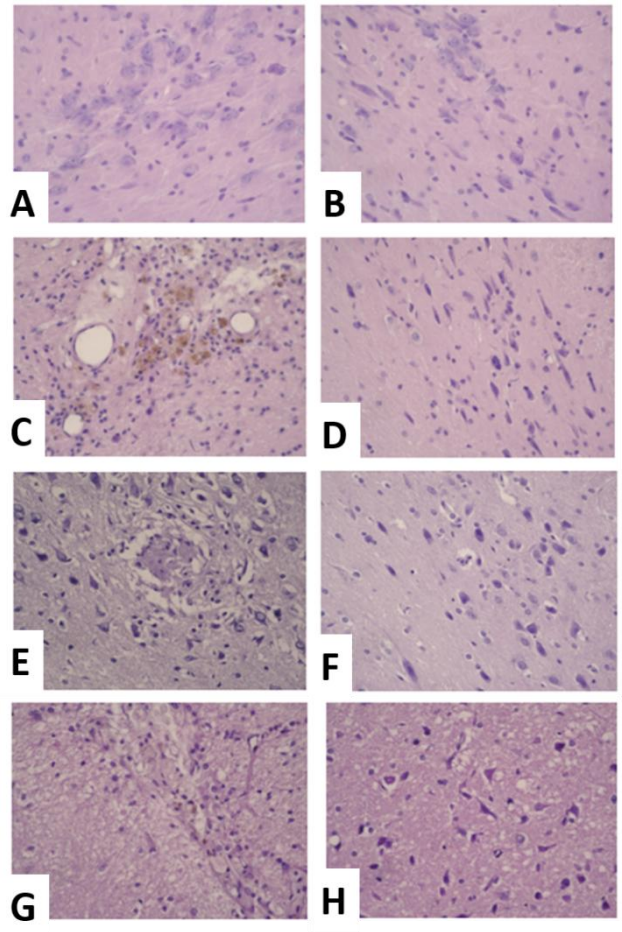

Fig.6. *Representative photomicrographs of the substantia nigra of the rat brain. H&E staining, magnification x400. A, B – intact animals; C, D – sham-operated animals; E, F – LPS-PD; G, H – LPS-PD + Zn64-asp.*

The neurons of the substantia nigra were significantly smaller as compared to those in intact animals, and dead hyperchromic neurons were detected. The median values of the neuron area in the *substantia nigra* of sham-operated rats was 283.5 [246.4 – 343.5] μm2 vs 500.4 [371.7 – 701.6] μm2 in the intact animals. In the LPS-PD group, the structural changes were similar to those in the sham-operated animals, but much more pronounced (Fig.6E and F). Edema and gliosis were observed in the area of toxin injection. The neurons in the substantia nigra were deformed, their perikaryon area was significantly smaller, and their number in the microsection projection was reduced as compared to both intact and sham-operated animals. The neuronal area was significantly smaller as compared to the values in the sham-operated group, with a median value of 204.0 [158.6 – 285.3] μm2 and 283.5 [246.4 – 343.5] μm2, respectively. In the LPS-lesioned rats received ^{64}Zn-asp, the number of neurons with relatively preserved perikaryons was higher than that in untreated animals (Fig.6G and H), which was reflected in morphometric parameters (a significant increase in neuronal area by 32.6%, $P<0.05$).

Intranigral LPS injection induced ~60% DN degeneration depicted by reduced immunoreactivity for TH (Fig. 7C).

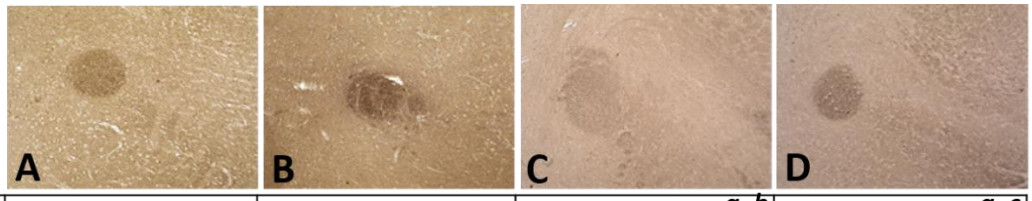

Q	3.0 ± 0.01	2.8 ± 0.04	1.1 ± 0.06$^{a, b}$	2.6 ± 0.08$^{a, c}$

Fig.7. *Representative immunohistochemical images of the TH-positive neurons (brown) in hippocampal area: intact animals (A), sham-operated animals (B), LPS-lesioned (C), LPS-PD + ^{64}Zn-asp, magnification x50. Quick scores (Q) under the images, calculated by multiplying the percentage of positive cells (P) by the intensity (I) and presented as: Q = P x I, are shown). Data are presented as mean ± SD. a - p ≤ 0.05 as compared*

to intact animals, b - $p \leq 0.05$ as compared to sham-operated animals; c - $p \leq 0.05$ as compared to LPS-PD group (ANOVA with Tukey's post-hoc test).

Q values in LPS-PD group were 3 times lower as compared to those in intact and sham-operated animals. Q values in LPS-lesioned rats treated with ^{64}Zn-asp (Fig. 7D) were comparable to those in sham-operated rats (Fig. 7A and B). DN loss was also confirmed by the results of apomorphine tests. On Day 8 (7 days after the surgery and day before the treatment initiation), contralateral rotation rate in LPS-injected rats was at the average 2.2 rpm indicating ~ 44-60% DN loss (Fig.8A). On Day 15 (14 days after surgery) 67% of the animals from LPS-PD group showed 23% increase of rotation rate indicating progressive DN loss (Fig.8A and B), whereas rotation rates of 33% of untreated animals with LPS-PD were unchanged or slightly decreased. In contrast, 86% of the rats from group LPS-PD + ^{64}Zn-asp demonstrated 13% decrease of rotation rate indicating preserving/restoring DN, whereas rotation rates in 14% of the animals from this group were unchanged or slightly increased indicating progressive DN loss.

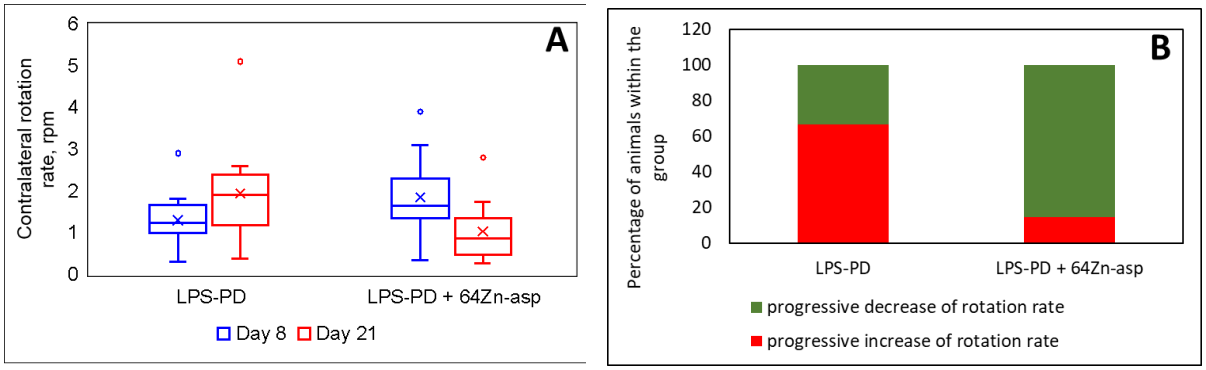

Fig.8. *Effect of Zn64-asp on apomorphine-induced rotation in LPS-lesioned rats. A – a mean rotation rate in the 1-st and 2-nd apomorphine test. Data are presented as medians and IQR. B - percentage of rats with an increase or decrease in rotation rate between the 1-st and 2-nd apomorphine test.*

We used open field test and EPM test for assessing behavioral functions in animals. DN loss in the LPS-lesioned rats was associated with behavioral alterations (Fig.9). Specifically, spontaneous locomotor activity of the LPS-lesioned rats was reduced as indicated by the decreased median value of total distance traveled in open field arena by 37% as compared to control groups ($p=0.06$) (Fig.9A), and in EPM-test - by 2.4 times as compared to control groups ($p \leq 0.05$) (Fig.9D). Treatment with ^{64}Zn-asp improved LPS-induced locomotor

activity impairment – median value of total distance traveled in rats from LPD-PD+^{64}Zn-asp group in both tests was higher than that in untreated animals and did not differ significantly from that in control groups.

By the end of the experiment, LPS-lesioned rats exhibited moderate anxiety-like behavior. The time spent in the inner perimeter of the open field arena by rats in the LPS-PD group was approximately 2.5 times lower than that of the control group ($p > 0.05$) (Fig. 9B). The time spent in squares bordered by two walls, indicative of thigmotaxis, was slightly higher in LPS-lesioned rats compared to the control group (Fig. 9C). The time spent in a stretched attend posture, which reflects risk assessment behavior, was more than twice as low in LPS-lesioned rats compared to control animals (Fig. 9E). In contrast, LPS-lesioned rats treated with 64Zn-asp exhibited behavior comparable to that of the control group across all these parameters. Rearing frequency was slightly reduced in animals from the LPS-PD group as compared to rats from control groups (Fig.9F). In animals with LPS-PD treated with ^{64}Zn-asp, a tendency towards normalizingthe rearing was observed. Taken together these results indicate that the treatment with ^{64}Zn-asp mitigates anxiogenic effects of LPS.

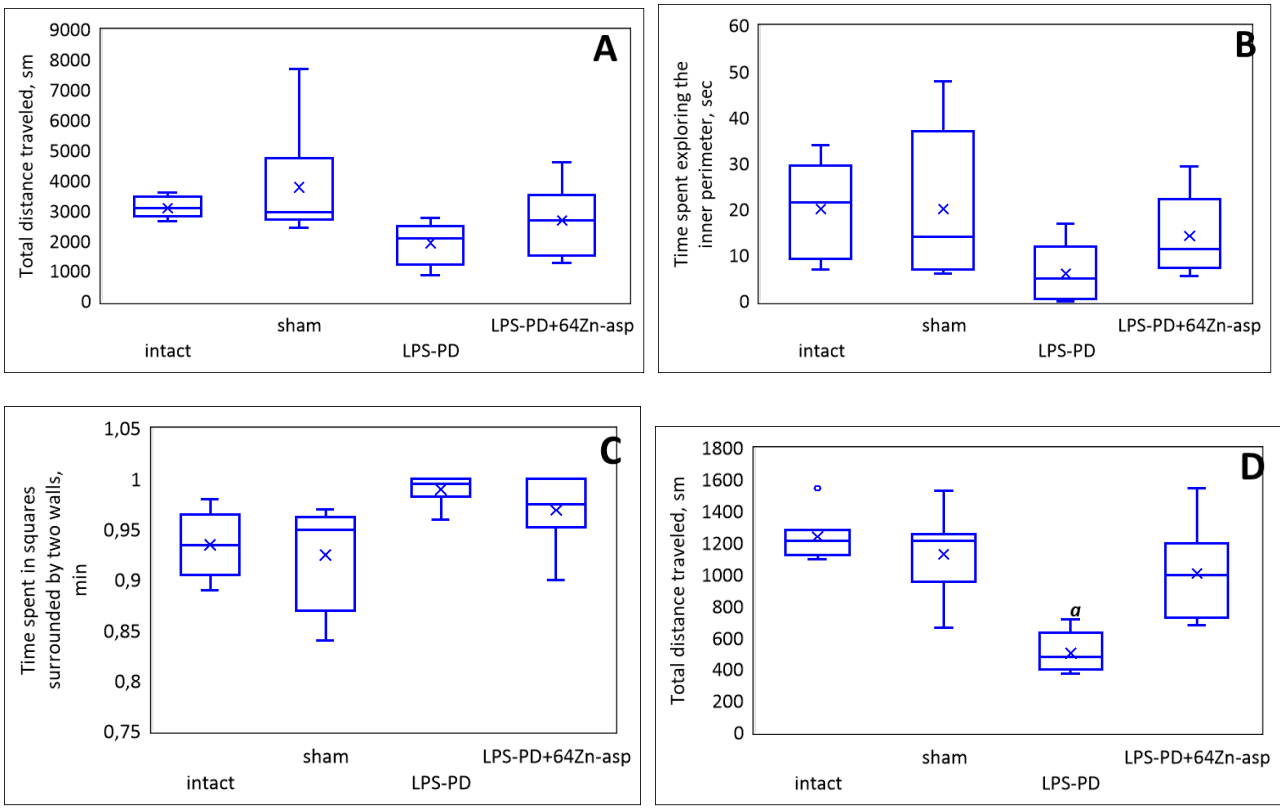

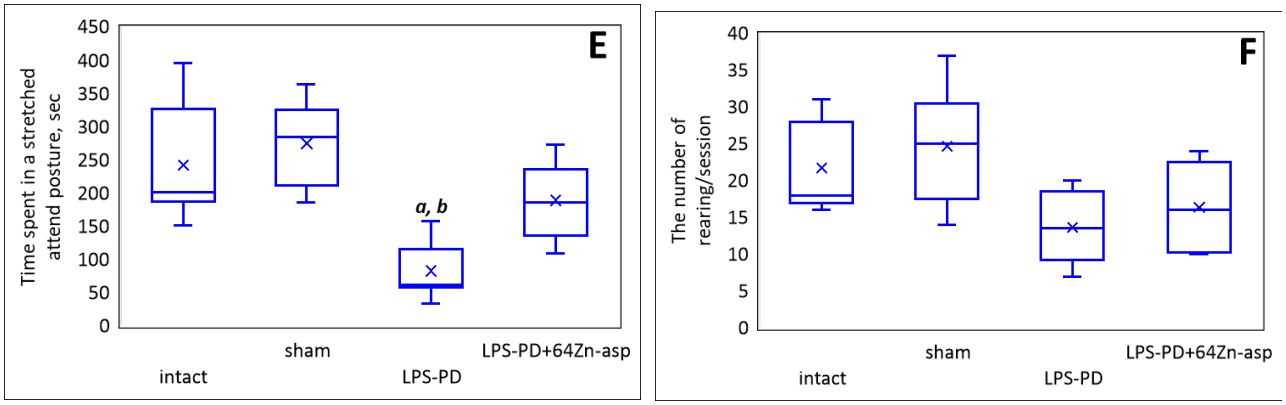

***Fig.9**. Effect of ^{64}Zn-asp on behavioral characteristics of LPS-lesioned rats. A – total distance traveled in open field test; B – time spent exploring the inner perimeter in open field test; C – thigmotaxis behavior in open field test; D - total distance traveled in EPM test; E – risk assessment behavior in EPM test; F – number of rearing in open field test. Data are presented as medians and IQR. a - $p \leq 0.05$ as compared to intact animals, b - $p \leq 0.05$ as compared to sham-operated animals; c - $p \leq 0.05$ as compared to LPS-PD group (Kruskal-Wallis's test).*

DISCUSSION

Over the past two decades, research has highlighted the significant role of neuroinflammation in the degeneration of the nigrostriatal dopaminergic pathway, a key pathological feature of PD. Recognizing the critical role of inflammation in the progression and persistence of PD could open new avenues for therapeutic strategies (Araújo et al., 2022; Grotemeyer et al., 2022). In this study, out of the many PD animal models we selected lipopolysaccharide (LPS)-induced one for exploring anti-inflammatory properties of a novel zinc-based compound. LPS-induced PD model is considered as one of the best so-called inflammatory or immune-related model. In addition, this model recapitulates many aspects of PD clinical picture including motor impairment and non-motor symptoms (García-Revilla et al., 2022; Deng et al., 2020; Oliynyk et al., 2023). LPS (endotoxin) is canonical microbe-associated molecular pattern and potent inflammogen, which nevertheless does not affect DN directly (Qin et al., 2004). Unilateral LPS injection into the *substantia nigra* elicits a robust neuroinflammatory response and subsequent loss of DN (Sanfeliu et al., 2024). LPS induces canonical NF-κB pathway (Guo et al., 2024). Zinc sulfate has been shown to inhibit LPS-induced inflammatory responses in microglial cells *in vitro* by interfering with NF-κB pathway through the up-regulation of A20 expression (Hongxia et al., 2019). This provided another reason for us to select LPS-induced PD model for studying the impact of novel zinc preparation on neuroinflammation and, as a result, on motor dysfunction in lesioned rats.

The form of zinc used in supplements or treatments can significantly impact its bioavailability and therapeutic effects. Over time, zinc supplements have evolved from inorganic to organic forms, largely to address one major limitation of inorganic zinc compounds: low bioavailability (Liu, 2023). The isotopically modified zinc employed in this study, ^{64}Zn-asp, offers an additional benefit, as the chelate complex of Zn^{2+} with aspartic acid has demonstrated allogenic suppressive activity, highlighting its potential for modulating inflammatory immune responses (Piacenza, 2023).

Neuroinflammation involves the activation of glial cells in the brain, primarily MG and astrocytes, which are tightly interconnected. In neurodegenerative diseases, their interaction is initiated by the binding of damage-associated molecular patterns (DAMPs) to Toll-like receptors (TLRs) on the membranes of MG and astrocytes or to intracellular receptors following endocytosis. This process activates downstream signaling pathways (Kam et al., 2020). Both MG and astrocytes can serve as the primary sensors of DAMPs. For example, the activation of TLR4 by α-synuclein in MG stimulates phagocytic activity, the release of pro-inflammatory cytokines, and the production of ROS, which in turn promotes the pro-inflammatory transformation of astrocytes. Additionally, α-synuclein binding to FcγRIIB on MG suppresses their phagocytic function by activating SHP-1, further inhibiting phagocytosis (Zhao et al., 2024). Among activated astrocytes, the pro-inflammatory phenotype intensifies the inflammatory activation of microglia. These astrocytes release a significant number of inflammatory mediators, contributing to excitotoxicity and exacerbating the inflammatory response (Sun et al., 2023). In LPS-lesioned rats in our experiments, reactive astrogliosis with a significant increase of MBP in brain homogenates was registered, indicating demyelination and neuronal damage (Kıray et al., 2016). The anti-inflammatory effect of ^{64}Zn-asp was evidenced by reducing of reactive astrogliosis, as was ascertained by a decrease in the level of GFAP and its breakdown products both in brain tissue homogenates and in blood serum, as well as by significant decrease in MBP in the brain homogenate. Reactive astrogliosis was associated with metabolic changes of MG. LPS is the most potent pro-inflammatory trigger for microglia/macrophages, that transform resting MG of M2 anti-inflammatory homeostatic profile to M1 polarized reactive cells (Allendorf et al., 2020). However, the functional state of the complex population microglia/macrophages in neuroinflammation does not fit within the simplified M1/M2 paradigm. First, inflamed MG contains cells with different profiles: M1 (classical activation), M2 (alternative activation or 'acquired deactivation') including intermediate phenotypes M2a, M2b, M2c. Second, as mentioned above, brain-resident phagocyte population contains MG and BAM. In adult, MG and BAM possess distinct functions in the brain. MG are self-renewed,

highly phagocytic and are mostly responsible for tissue homeostasis maintenance by scavenging cell debris and synapses, mediating neurogenesis in central nervous system injury etc. BAM are answerable for the immune surveillance of pathological antigens and endowed with increased antigen-presenting capacity with CD86 overexpression. Principal phenotypic marker differentiating MG and BAM is CD206. Resting MG is $CD206^{-}$, reactive MG is $CD206^{low}$. BAM are $CD206^{high}$ (Wen et al., 2024; Sun & Jiang 2024). Single stereotaxic LPS injection was reported to increase accumulating cytoplasmic α-synuclein in nigral TH positive neurons (Choi et al., 2009; Deng et al., 2020). $CD206^{-}$ MG are vital in scavenging α-synuclein. However, excessive α-synuclein production could overwhelm its scavenging and consequently, can increase extracellular α-synuclein protein. As stated above, extracellular α-synuclein acts as DAMPs for MG inducing the NFκB signaling pathway through TLR, and transforming resting cells into reactive, that is accompanied by blocking MG phagocytic activity and a decrease of α-synuclein clearing (Miao and Meng, 2024). In our experiments, treatment of LPS-lesioned rats with ^{64}Zn-asp was accompanied by significant increase of microglia/macrophage phagocytic activity, in such a way restoring homeostatic scavenging capacity of these cells, that in turn could facilitate the resolution of neuroinflammation. In addition, treatment with ^{64}Zn-asp was associated with a decrease of CD86+ and CD206+ cell count. Given that BAM subset mostly represents CD86+ and CD206+ cell fractions in the complex microglia/macrophage population and may be replenished by the circulating monocytes during inflammation; this effect may be explained by inhibitory effect of ^{64}Zn-asp on inflammatory blood cell recruitment.

Reduced neuroinflammation in rats with LPS-PD that received the i.v. ^{64}Zn-asp treatment was correlated with moderately reduced manifestation of motor and non-motor symptoms of the disease. The treatment course of i.v. ^{64}Zn-asp injections mitigated weight loss, alleviated anxiety-like behavior, and reduced locomotor activity impairment. Weight loss in animal PD models is partly related to anxiety-like behavior, which (along with impairment of locomotor activity) is in turn associated with loss of dopaminergic and serotonergic neurons. The improvement in motor and non-motor symptoms observed in LPS-lesioned rats treated with ^{64}Zn-asp can likely be attributed to the prevention of dopaminergic neuron (DN) loss and/or their restoration. This conclusion is supported by the findings from the histological analysis, the apomorphine test, and immunostaining for tyrosine hydroxylase (TH). Increased blood-brain barrier permeability, caused by LPS-induced inflammation (Jangula and Murphy, 2013), allowed zinc movement to the brain tissues. The reduction in DN loss in the ^{64}Zn-asp treated animals may be the result of the anti-inflammatory effect of ^{64}Zn-asp aimed at restraining the pro-

inflammatory and neuroprotective profile of microglia/macrophages and astroglia involved in neuroinflammation. On the other hand, considering that zinc regulates cell proliferation (Fan et al., 2024), attenuated DN loss in treated animals could be attributed to the stimulated proliferation and differentiation of neural stem cells.

In conclusion, neuroinflammation is recognized as a critical factor in the PD pathogenesis. Given the global prevalence of neuroinflammation as a condition commonly associated with PD, the development of anti-inflammatory therapies remains highly relevant. In our study, LPS-PD in rats was characterized by neuroinflammation, evidenced by reactive astrogliosis and pro-inflammatory metabolic shift in MG/BAM cells. Intravenous administration of ^{64}Zn-asp effectively inhibited neuroinflammation, resulting in a beneficial impact on cognitive measures in the affected animals. However, it is important to note that this study did not evaluate the direct effects of ^{64}Zn-asp on zinc homeostasis or neuronal function, leaving certain aspects of the drug's action unexamined and necessitating further research. Despite this limitation, the results support the potential use of ^{64}Zn-asp as a therapeutic agent to mitigate inflammation and enhance cognitive function in PD.

ACKNOWLEDGEMENTS

The study was supported by a TSNUK project N 18DP36-10.

REFERENCES

Adam, H., Gopinath, S.C.B., Md Arshad, M.K., Adam, T., Parmin, N.A., Husein, I., Hashim, U., 2023. An update on pathogenesis and clinical scenario for Parkinson's disease: diagnosis and treatment. 3 Biotech. 13 (5), 142. https://doi.org/10.1007/s13205-023-03553-8.

Alam, A., Hana, Z., Jin, Z., Suen, K. C., & Ma, D. (2018). Surgery, neuroinflammation and cognitive impairment. EBioMedicine, 37, 547–556. https://doi.org/10.1016/j.ebiom.2018.10.021

Al-Harthi, S., Kharchenko, V., Mandal, P., Gourdoupis, S., Jaremko, Ł., 2022. Zinc ions prevent α-synuclein aggregation by enhancing chaperone function of human serum albumin. Int J Biol Macromol. 222 (Pt B), 2878-2887. https://doi.org/10.1016/j.ijbiomac.2022.10.066.

Albarede, F., Télouk, P., Balter, V., Bondanese, V.P., Albalat, E., Oger, P., Bonaventura, P., Miossec, P., Fujii, T., 2016. Medical applications of Cu, Zn, and S isotope effects. Metallomics. 8 (10), 1056-1070. https://doi.org/10.1039/c5mt00316d.

Alfaidi, M., Barker, R. A., & Kuan, W. L. (2024). An update on immune-based alpha-synuclein trials in Parkinson's disease. Journal of neurology, 272(1), 21. https://doi.org/10.1007/s00415-024-12770-x

Allendorf, D.H., Franssen, E.H., Brown, G.C., 2020. Lipopolysaccharide activates microglia via neuraminidase 1 desialylation of Toll-like Receptor 4. J Neurochem. 155 (4), 403-416. https://doi.org/10.1111/jnc.15024.

Araújo, B., Caridade-Silva, R., Soares-Guedes, C., Martins-Macedo, J., Gomes, E. D., Monteiro, S., & Teixeira, F. G. (2022). Neuroinflammation and Parkinson's Disease-From Neurodegeneration to Therapeutic Opportunities. Cells, 11(18), 2908. https://doi.org/10.3390/cells11182908

Badawoud, A. M., Ali, L. S., Abdallah, M. S., El Sabaa, R. M., Bahaa, M. M., Elmasry, T. A., Wahsh, E., Yasser, M., Eltantawy, N., Eldesoqui, M., & Hamouda, M. A. (2024). The relation between Parkinson's disease and non-steroidal anti-inflammatories; a systematic review and meta-analysis. Frontiers in pharmacology, 15, 1434512. https://doi.org/10.3389/fphar.2024.1434512

Baltaci, S. B., Gümüş, H., Ünal, Ö., Acar, G., & Bayiroğlu, A. F. (2024). Zinc Supplementation Improves ZIP14 (SLC39A14) Levels in Cerebral Cortex Suppressed by icv-STZ Injection. Noro psikiyatri arsivi, 61(1), 11–14. https://doi.org/10.29399/npa.28426

Berg, D., Eggert, K., Haslinger, B., Kassubek, J., Mollenhauer, B., Reetz, K., Rogge, A., Schaeffer, E., Tönges, L., & Zeuner, K. E. (2020). Disease modifying treatment trials in Parkinson's disease: how to balance expectations and interests of patients, physicians and industry partners?. Neurological research and practice, 2, 31. https://doi.org/10.1186/s42466-020-00076-y

Briassoulis, G., Briassoulis, P., Ilia, S., Miliaraki, M., & Briassouli, E. (2023). The Anti-Oxidative, Anti-Inflammatory, Anti-Apoptotic, and Anti-Necroptotic Role of Zinc in COVID-19 and Sepsis. Antioxidants (Basel, Switzerland), 12(11), 1942. https://doi.org/10.3390/antiox12111942

Brown D. R. (2009). Metal binding to alpha-synuclein peptides and its contribution to toxicity. Biochemical and biophysical research communications, 380(2), 377–381. https://doi.org/10.1016/j.bbrc.2009.01.103

Buesa, R.J., Peshkov, M.V., 2011. Complete elimination of xylene in practice of a histology laboratory. Arkh Patol. 73, 54–60.

Chan, Y., Walmsley, R.P., 1997. Learning and understanding the Kruskal-Wallis one-way analysis-of-variance-by-ranks test for differences among three or more independent groups. Phys Ther. 77 (12), 1755-1762. https://doi.org/10.1093/ptj/77.12.1755.

Chen, C., Turnbull, D.M., Reeve, A.K., 2019. Mitochondrial Dysfunction in Parkinson's Disease-Cause or Consequence? Biology (Basel). 8 (2), 38. https://doi.org/10.3390/biology8020038.

Choi, D.Y., Liu, M., Hunter, R.L., Cass, W.A., Pandya, J.D., Sullivan, P.G., Shin, E.J., Kim, H.C., Gash, D.M., Bing, G., 2009. Striatal neuroinflammation promotes Parkinsonism in rats. PLoS One. 4 (5), e5482. https://doi.org/10.1371/journal.pone.0005482.

Cornice, J., Verzella, D., Arboretto, P., Vecchiotti, D., Capece, D., Zazzeroni, F., & Franzoso, G. (2024). NF-κB: Governing Macrophages in Cancer. Genes, 15(2), 197. https://doi.org/10.3390/genes15020197

Cumming, K., Macleod, A.D., Myint, P.K., Counsell, C.E., 2017. Early weight loss in parkinsonism predicts poor outcomes: Evidence from an incident cohort study. Neurology. 89 (22), 2254-2261. https://doi.org/10.1212/WNL.0000000000004691.

Çınar, E., Tel, B. C., & Şahin, G. (2022). Neuroinflammation in Parkinson's Disease and its Treatment Opportunities. Balkan medical journal, 39(5), 318–333. https://doi.org/10.4274/balkanmedj.galenos.2022.2022-7-100

Cvijanovich, N. Z., King, J. C., Flori, H. R., Gildengorin, G., Vinks, A. A., & Wong, H. R. (2016). Safety and Dose Escalation Study of Intravenous Zinc Supplementation in Pediatric Critical Illness. JPEN. Journal of parenteral and enteral nutrition, 40(6), 860–868. https://doi.org/10.1177/0148607115572193

Deng, I., Corrigan, F., Zhai, G., Zhou, X.F., Bobrovskaya, L., 2020. Lipopolysaccharide animal models of Parkinson's disease: Recent progress and relevance to clinical disease. Brain Behav Immun Health. 4, 100060. https://doi.org/10.1016/j.bbih.2020.100060.

de Vargas, L. D. S., Jantsch, J., Fontoura, J. R., Dorneles, G. P., Peres, A., & Guedes, R. P. (2023). Effects of Zinc Supplementation on Inflammatory and Cognitive Parameters in Middle-Aged Women with Overweight or Obesity. Nutrients, 15(20), 4396. https://doi.org/10.3390/nu15204396

Falkeholm, L., Grant, C.A., Magnusson, A., Mollur, E., 2001. Xylene-free method for histological preparation: A Multicentre Evaluation. Lab Invest. 81 (9), 1213-1221. https://doi.org/10.1038/labinvest.3780335.

Fan, Y.G., Wu, T.Y., Zhao, L.X., Jia, R.J., Ren, H., Hou, W.J., Wang, Z.Y., 2024. From zinc homeostasis to disease progression: Unveiling the neurodegenerative puzzle. Pharmacol Res. 199, 107039. https://doi.org/10.1016/j.phrs.2023.107039.

Feijó, G. D. S., Jantsch, J., Correia, L. L., Eller, S., Furtado-Filho, O. V., Giovenardi, M., Porawski, M., Braganhol, E., & Guedes, R. P. (2022). Neuroinflammatory responses following zinc or branched-chain amino acids supplementation in obese rats. Metabolic brain disease, 37(6), 1875–1886. https://doi.org/10.1007/s11011-022-00996-5

Fernández-Espejo, E., Rodríguez de Fonseca, F., Gavito, A. L., Córdoba-Fernández, A., Chacón, J., & Martín de Pablos, Á. (2022). Myeloperoxidase and Advanced Oxidation Protein Products in the Cerebrospinal Fluid in Women and Men with Parkinson's Disease. Antioxidants (Basel, Switzerland), 11(6), 1088. https://doi.org/10.3390/antiox11061088

Frank, M.G., Wieseler-Frank, J.L., Watkins, L.R., Maier, S.F., 2006. Rapid isolation of highly enriched and quiescent microglia from adult rat hippocampus: immunophenotypic and functional characteristics. J. Neurosci. Methods. 151 (2), 121–130. https://doi.org/10.1016/j.jneumeth.2005.06.026.

Forloni, G., La Vitola, P., Cerovic, M., & Balducci, C. (2021). Inflammation and Parkinson's disease pathogenesis: Mechanisms and therapeutic insight. Progress in molecular biology and translational science, 177, 175–202. https://doi.org/10.1016/bs.pmbts.2020.11.001

Gage, G.J., Kipke, D.R., Shain, W., 2012. Whole animal perfusion fixation for rodents. J Vis Exp. 30, 65. https://doi.org/10.3791/3564.

Gammoh, N. Z., & Rink, L. (2017). Zinc in Infection and Inflammation. Nutrients, 9(6), 624. https://doi.org/10.3390/nu9060624

García-Revilla, J., Herrera, A.J., de Pablos, R.M., Venero, J.L., 2022. Inflammatory Animal Models of Parkinson's Disease. J Parkinsons Dis. 12 (s1), S165-S182. https://doi.org/10.3233/JPD-213138.

Grotemeyer, A., McFleder, R. L., Wu, J., Wischhusen, J., & Ip, C. W. (2022). Neuroinflammation in Parkinson's Disease - Putative Pathomechanisms and Targets for Disease-Modification. Frontiers in immunology, 13, 878771. https://doi.org/10.3389/fimmu.2022.878771

Gumus, H., Baltaci, S. B., Unal, O., Gulbahce-Mutlu, E., Mogulkoc, R., & Baltaci, A. K. (2023). Zinc Ameliorates Nogo-A Receptor and Osteocalcin Gene Expression in Memory-Sensitive Rat Hippocampus Impaired by Intracerebroventricular Injection of Streptozotocin. Biological trace element research, 201(7), 3381–3386. https://doi.org/10.1007/s12011-022-03410-4

Guo, Q., Jin, Y., Chen, X., Ye, X., Shen, X., Lin, M., Zeng, C., Zhou, T., & Zhang, J. (2024). NF-κB in biology and targeted therapy: new insights and translational implications. Signal transduction and targeted therapy, 9(1), 53. https://doi.org/10.1038/s41392-024-01757-9

Hafez, L. M., Aboudeya, H. M., Matar, N. A., El-Sebeay, A. S., Nomair, A. M., El-Hamshary, S. A., Nomeir, H. M., & Ibrahim, F. A. R. (2023). Ameliorative effects of zinc supplementation on cognitive function and hippocampal leptin signaling pathway in obese male and female rats. Scientific reports, 13(1), 5072. https://doi.org/10.1038/s41598-023-31781-8

Hoban, D.B., Connaughton, E., Connaughton, C., Hogan, G., Thornton, C., Mulcahy, P., Moloney, T.C., Dowd, E., 2013. Further characterisation of the LPS model of Parkinson's disease: a comparison of intra-nigral and intra-striatal lipopolysaccharide administration on motor function, microgliosis and nigrostriatal neurodegeneration in the rat. Brain Behav. Immun. 27 (1), 91–100. https://doi.org/ 10.1016/j.bbi.2012.10.001.

Hommel, A. L. A. J., Krijthe, J. H., Darweesh, S., & Bloem, B. R. (2022). The association of comorbidity with Parkinson's disease-related hospitalizations. Parkinsonism & related disorders, 104, 123–128. https://doi.org/10.1016/j.parkreldis.2022.10.012

Hongxia, L., Yuxiao, T., Zhilei, S., Yan, S., Yicui, Q., Jiamin, S., Xin, X., Jianxin, Y., Fengfeng, M., & Hui, S. (2019). Zinc inhibited LPS-induced inflammatory responses by upregulating A20 expression in microglia BV2 cells. Journal of affective disorders, 249, 136–142. https://doi.org/10.1016/j.jad.2019.02.041

Jangula, A., Murphy, E.J., 2013. Lipopolysaccharide-induced blood brain barrier permeability is enhanced by alpha-synuclein expression. Neurosci Lett. 551, 23-27. https://doi.org/10.1016/j.neulet.2013.06.058.

Jaouen, K., Pouilloux, L., Balter, V., Pons, M.L., Hublin, J.J., Albarède, F., 2019. Dynamic homeostasis modeling of Zn isotope ratios in the human body. Metallomics. 11 (6), 1049-1059. https://doi.org/10.1039/c8mt00286j.

Jarosz, M., Olbert, M., Wyszogrodzka, G., Młyniec, K., & Librowski, T. (2017). Antioxidant and anti-inflammatory effects of zinc. Zinc-dependent NF-κB signaling. Inflammopharmacology, 25(1), 11–24. https://doi.org/10.1007/s10787-017-0309-4

Kam, T. I., Hinkle, J. T., Dawson, T. M., & Dawson, V. L. (2020). Microglia and astrocyte dysfunction in parkinson's disease. Neurobiology of disease, 144, 105028. https://doi.org/10.1016/j.nbd.2020.105028

Khrieba, M. O., Hegazy, S. K., Mustafa, W., & El-Haggar, S. M. (2024). Repurposing celecoxib as adjuvant therapy in patients with Parkinsonian disease: a new therapeutic dawn: randomized controlled pilot study. Inflammopharmacology, 32(6), 3729–3738. https://doi.org/10.1007/s10787-024-01567-z

Kiouri, D.P., Tsoupra, E., Peana, M., Perlepes, S.P., Stefanidou, M.E., Chasapis, C.T., 2023. Multifunctional role of zinc in human health: an update. EXCLI J. 22, 809-827. https://doi.org/10.17179/excli2023-6335.

Kıray, H., Lindsay, S.L., Hosseinzadeh, S., Barnett, S.C., 2016. The multifaceted role of astrocytes in regulating myelination. Exp Neurol. 283 (Pt B), 541-549. https://doi.org/10.1016/j.expneurol.2016.03.009.

Kisucká, A., Bimbová, K., Bačová, M., Gálik, J., & Lukáčová, N. (2021). Activation of Neuroprotective Microglia and Astrocytes at the Lesion Site and in the Adjacent Segments Is Crucial for Spontaneous Locomotor Recovery after Spinal Cord Injury. Cells, 10(8), 1943. https://doi.org/10.3390/cells10081943

Kwon, H. S., & Koh, S. H. (2020). Neuroinflammation in neurodegenerative disorders: the roles of microglia and astrocytes. Translational neurodegeneration, 9(1), 42. https://doi.org/10.1186/s40035-020-00221-2

Lamprea, M.R., Cardenas, F.P., Setem, J., Morato, S., 2008. Thigmotactic responses in an open-field. Braz J Med Biol Res. 41 (2), 135-140. https://doi.org/10.1590/s0100-879x2008000200010.

Leite-Almeida, H., Almeida-Torres, L., Mesquita, A.R., Pertovaara, A., Sousa, N., Cerqueira, J.J., Almeida, A., 2009. The impact of age on emotional and cognitive behaviours triggered by experimental neuropathy in rats. Pain. 144 (1-2), 57-65. https://doi.org/10.1016/j.pain.2009.02.024.

Lee, Y., Lee, S., Chang, S.C., Lee, J., 2019. Significant roles of neuroinflammation in Parkinson's disease: therapeutic targets for PD prevention. Arch Pharm Res. 42 (5), 416-425. https://doi.org/10.1007/s12272-019-01133-0.

Liddelow, S.A., Guttenplan, K.A., Clarke, L.E., Bennett, F.C., Bohlen, C.J., Schirmer, L., Bennett, M.L., Münch, A.E., Chung, W.S., Peterson, T.C., Wilton, D.K., Frouin, A., Napier, B.A., Panicker, N., Kumar, M., Buckwalter, M.S., Rowitch, D.H., Dawson, V.L., Dawson, T.M., Stevens, B., Barres, B.A., 2017. Neurotoxic reactive astrocytes are induced by activated microglia. Nature. 541 (7638), 481-487. https://doi.org/10.1038/nature21029.

Liu, S., Wang, N., Long, Y., Wu, Z., Zhou, S., 2023. Zinc Homeostasis: An Emerging Therapeutic Target for Neuroinflammation Related Diseases. Biomolecules. 13 (3), 416. https://doi.org/10.3390/biom13030416.

Mbiydzenyuy, N.E., Ninsiima, H.I., Valladares, M.B., Pieme, C.A., 2018. Zinc and linoleic acid pre-treatment attenuates biochemical and histological changes in the midbrain of rats with rotenone-induced Parkinsonism. BMC Neurosci. 19 (1), 29. https://doi.org/10.1186/s12868-018-0429-9.

Miao, Y., Meng, H., 2024. The involvement of α-synucleinopathy in the disruption of microglial homeostasis contributes to the pathogenesis of Parkinson's disease. Cell Commun Signal. 22 (1), 31. https://doi.org/10.1186/s12964-023-01402-y.

Mishra, P., Pandey, C. M., Singh, U., Gupta, A., Sahu, C., Keshri, A., 2019. Descriptive statistics and normality tests for statistical data. Ann. Card. Anaesth. 22 (1), 67–72. https://doi.org/10.4103/aca.ACA_157_18.

Mousaviyan, R., Davoodian, N., Alizadeh, F., Ghasemi-Kasman, M., Mousavi, S. A., Shaerzadeh, F., & Kazemi, H. (2021). Zinc Supplementation During Pregnancy Alleviates Lipopolysaccharide-Induced Glial Activation and Inflammatory Markers Expression in a Rat Model of Maternal Immune Activation. Biological trace element research, 199(11), 4193–4204. https://doi.org/10.1007/s12011-020-02553-6

Moynier, F., Borgne, M.L., Lahoud, E., Mahan, B., Mouton-Liger, F., Hugon, J., Paquet, C., 2020. Copper and zinc isotopic excursions in the human brain affected by Alzheimer's disease. Alzheimers Dement (Amst). 12 (1), e12112. https://doi.org/10.1002/dad2.12112.

Murakami, H., Shiraishi, T., Umehara, T., Omoto, S., & Iguchi, Y. (2023). Recent Advances in Drug Therapy for Parkinson's Disease. Internal medicine (Tokyo, Japan), 62(1), 33–42. https://doi.org/10.2169/internalmedicine.8940-21

Mussbacher, M., Derler, M., Basílio, J., & Schmid, J. A. (2023). NF-κB in monocytes and macrophages - an inflammatory master regulator in multitalented immune cells. Frontiers in immunology, 14, 1134661. https://doi.org/10.3389/fimmu.2023.1134661

Nakamura, R., Tomizawa, I., Iwai, A., Ikeda, T., Hirayama, K., Chiu, Y. W., Suzuki, T., Tarutani, A., Mano, T., Iwata, A., Toda, T., Sohma, Y., Kanai, M., Hori, Y., & Tomita, T. (2023). Photo-oxygenation of histidine residue inhibits α-synuclein aggregation. FASEB journal : official publication of the Federation of American Societies for Experimental Biology, 37(12), e23311. https://doi.org/10.1096/fj.202301533R

Nash, B., Ioannidou, K., Barnett, S.C., 2011. Astrocyte phenotypes and their relationship to myelination. J Anat. Jul. 219 (1), 44-52. https://doi.org/10.1111/j.1469-7580.2010.01330.x

Niu, C., Zou, Y., Dong, M., & Niu, Y. (2025). Plant-derived compounds as potential neuroprotective agents in Parkinson's disease. Nutrition (Burbank, Los Angeles County, Calif.), 130, 112610. https://doi.org/10.1016/j.nut.2024.112610

Novak, P., Temnikov, M., Balakin O. Pharmaceutical composition for improving health, cure abnormalities and degenerative disease, achieve anti-aging effect of therapy and therapeutic effect on mammals and method thereof. Pharmaceutical Composition for Improving Health, Cure. 2022. https://patents.google.com/patent/US20200000845A1/en

Novak, P., Balakin, A., Temnik, M., 2022. In Vitro Anticancer Activity of the Light Stable Zinc Isotope (64Zn) Compounds. Anticancer Res. 42 (12), 5685-5698. https://doi.org/10.21873/anticanres.16077.

Oliynyk, Z., Rudyk, M., Dovbynchuk, T., Dzubenko, N., Tolstanova, G., Skivka, L. 2023. Inflammatory hallmarks in 6-OHDA- and LPS-induced Parkinson's disease in rats. Brain Behav Immun Health. 30, 100616. https://doi.org/10.1016/j.bbih.2023.100616.

Olson, K. E., Abdelmoaty, M. M., Namminga, K. L., Lu, Y., Obaro, H., Santamaria, P., Mosley, R. L., & Gendelman, H. E. (2023). An open-label multiyear study of sargramostim-treated Parkinson's disease patients examining drug safety, tolerability, and immune biomarkers from limited case numbers. Translational neurodegeneration, 12(1), 26. https://doi.org/10.1186/s40035-023-00361-1

Pardo-Moreno, T., García-Morales, V., Suleiman-Martos, S., Rivas-Domínguez, A., Mohamed-Mohamed, H., Ramos-Rodríguez, J. J., Melguizo-Rodríguez, L., & González-Acedo, A. (2023). Current Treatments and New, Tentative Therapies for Parkinson's Disease. Pharmaceutics, 15(3), 770. https://doi.org/10.3390/pharmaceutics15030770

Pauletti, G., Dandekar, S., Rong, H., Ramos, L., Peng, H., Seshadri, R., Slamon, D.J., 2000. Assessment of methods for tissue-based detection of the HER-2/neu alteration in human breast cancer: a direct comparison of fluorescence in situ hybridization and immunohistochemistry. J. Clin. Oncol. 18 (21), 3651–6364. https://doi.org/10.1200/JCO.2000.18.21.3651.

Paxinos, G., Watson, C., 1982. The rat brain in stereotaxic coordinats. Academic Press.

Pérez S., Rius-Pérez S. (2022). Macrophage Polarization and Reprogramming in Acute Inflammation: A Redox Perspective. Antioxidants (Basel, Switzerland), 11(7), 1394. https://doi.org/10.3390/antiox11071394

Piacenza, F., Giacconi, R., Costarelli, L., & Malavolta, M. (2023). Preliminary Comparison of Fractional Absorption of Zinc Sulphate, Zinc Gluconate, and Zinc Aspartate after Oral Supplementation in Healthy Human Volunteers. Nutrients, 15(8), 1885. https://doi.org/10.3390/nu15081885

Prasad A. S. (2014). Zinc is an Antioxidant and Anti-Inflammatory Agent: Its Role in Human Health. Frontiers in nutrition, 1, 14. https://doi.org/10.3389/fnut.2014.00014

Qin, L., Liu, Y., Wang, T., Wei, S. J., Block, M. L., Wilson, B., Liu, B., & Hong, J. S. (2004). NADPH oxidase mediates lipopolysaccharide-induced neurotoxicity and proinflammatory gene expression in activated microglia. The Journal of biological chemistry, 279(2), 1415–1421. https://doi.org/10.1074/jbc.M307657200

Ramis, R., Ortega-Castro, J., Vilanova, B., Adrover, M., & Frau, J. (2018). A Systematic DFT Study of Some Plausible Zn(II) and Al(III) Interaction Sites in N-Terminally Acetylated α-Synuclein. The journal of physical chemistry. A, 122(2), 690–699. https://doi.org/10.1021/acs.jpca.7b10744

Rudyk, M.P., Pozur, V.V., Voieikova, D.O., Hurmach, Y.V., Khranovska, N.M., Skachkova, O.V., Svyatetska, V.M., Fedorchuk, O.G., Skivka, L.M., Berehova, T.V., Ostapchenko, L.I., 2018. Sex-based differences in phagocyte metabolic profile in rats with monosodium glutamate-induced obesity. Sci. Rep. 8 (1), 5419. https://doi.org/10.1038/s41598-018-23664-0.

Safiri, S., Noori, M., Nejadghaderi, S.A., Mousavi, S.E., Sullman, M.J.M., Araj-Khodaei, M., Singh, K., Kolahi, A.A., Gharagozli, K., 2023. The burden of Parkinson's disease in the Middle East and North Africa region, 1990-2019: results from the global burden of disease study 2019. BMC Public Health. 23 (1), 107. https://doi.org/10.1186/s12889-023-15018-x.

Sanfeliu, C., Bartra, C., Suñol, C., & Rodríguez-Farré, E. (2024). New insights in animal models of neurotoxicity-induced neurodegeneration. Frontiers in neuroscience, 17, 1248727. https://doi.org/10.3389/fnins.2023.1248727

Saini, N., Schaffner, W., 2010. Zinc supplement greatly improves the condition of parkin mutant Drosophila. Biol Chem. 391 (5), 513-518. https://doi.org/10.1515/BC.2010.052.

Sameei, P., Fatehfar, S., Abdollahzadeh, N., Chodari, L., Saboory, E., & Roshan-Milani, S. (2023). The effects of forced exercise and zinc supplementation during pregnancy on prenatally stress-induced behavioral and neurobiological consequences in adolescent female rat offspring. Developmental psychobiology, 65(6), e22411. https://doi.org/10.1002/dev.22411

Sestakova, N., Puzserova, A., Kluknavsky, M., Bernatova, I., 2013. Determination of motor activity and anxiety-related behaviour in rodents: methodological aspects and role of nitric oxide. Interdiscip Toxicol. 6 (3), 126-135. https://doi.org/10.2478/intox-2013-0020.

Silvin, A., Qian, J., Ginhoux, F., 2023. Brain macrophage development, diversity and dysregulation in health and disease. Cell Mol Immunol. 20 (11), 1277-1289. https://doi.org/10.1038/s41423-023-01053-6.

Solovyev, N., El-Khatib, A.H., Costas-Rodríguez, M., Schwab, K., Griffin, E., Raab, A., Platt, B., Theuring, F., Vogl, J., Vanhaecke, F., 2021. Cu, Fe, and Zn isotope ratios in murine Alzheimer's disease models suggest specific signatures of amyloidogenesis and tauopathy. J Biol Chem. 296, 100292. https://doi.org/10.1016/j.jbc.2021.100292.

Song, J., Zhao, Y., Shan, X., Luo, Y., Hao, N., & Zhao, L. (2024). Active ingredients of Chinese medicine with immunomodulatory properties: NF-κB pathway and Parkinson's disease. Brain research, 1822, 148603. https://doi.org/10.1016/j.brainres.2023.148603

Squitti, R., Pal, A., Picozza, M., Avan, A., Ventriglia, M., Rongioletti, M. C., & Hoogenraad, T. (2020). Zinc Therapy in Early Alzheimer's Disease: Safety and Potential Therapeutic Efficacy. Biomolecules, 10(8), 1164. https://doi.org/10.3390/biom10081164

Sun, M., You, H., Hu, X., Luo, Y., Zhang, Z., Song, Y., An, J., & Lu, H. (2023). Microglia-Astrocyte Interaction in Neural Development and Neural Pathogenesis. Cells, 12(15), 1942. https://doi.org/10.3390/cells12151942

Sun, R., Jiang, H., 2024. Border-associated macrophages in the central nervous system. Clin Immunol. 109921. https://doi.org/10.1016/j.clim.2024.109921.

Talanov, S.A., Oleshko, N.N., Tkachenko, M.N., Sagach, V.F., 2006. Pharmacoprotective influences on different links of the mechanism underlying 6-hydroxydopamineinduced degeneration of nigro-striatal dopaminergic neurons. Neurophysiology. 38 (2), 128–133. https://doi.org/10.1007/s11062-006-0035-9.

Tanaka, Y.K., Hirata, T., 2018. Stable Isotope Composition of Metal Elements in Biological Samples as Tracers for Element Metabolism. Anal Sci. 34 (6), 645-655. https://doi.org/10.2116/analsci.18SBR02.

Troncoso-Escudero, P., Parra, A., Nassif, M., & Vidal, R. L. (2018). Outside in: Unraveling the Role of Neuroinflammation in the Progression of Parkinson's Disease. Frontiers in neurology, 9, 860. https://doi.org/10.3389/fneur.2018.00860

Walf, A.A., Frye, C.A., 2007. The use of the elevated plus maze as an assay of anxiety-related behavior in rodents. Nat Protoc. 2 (2), 322-328. https://doi.org/10.1038/nprot.2007.44.

Walsh, S., Finn, D.P., Dowd, E., 2011. Time-course of nigrostriatal neurodegeneration and neuroinflammation in the 6-hydroxydopamine-induced axonal and terminal lesion models of Parkinson's disease in the rat. Neuroscience 175, 251–261. https:// doi.org/10.1016/j.neuroscience.2010.12.005.

Wang, J., He, W., Zhang, J., 2023. A richer and more diverse future for microglia phenotypes. Heliyon. 9 (4), e14713. https://doi.org/10.1016/j.heliyon.2023.e14713.

Wen, W., Cheng, J., Tang, Y., 2024. Brain perivascular macrophages: current understanding and future prospects. Brain. 147 (1), 39-55. https://doi.org/10.1093/brain/awad304.

Wessels, I., Maywald, M., & Rink, L. (2017). Zinc as a Gatekeeper of Immune Function. Nutrients, 9(12), 1286. https://doi.org/10.3390/nu9121286

Willis, A.W., Roberts, E., Beck, J.C., Fiske, B., Ross, W., Savica, R., Van Den Eeden, S.K., Tanner, C.M., Marras, C., 2022. Parkinson's Foundation P4 Group. Incidence of Parkinson disease in North America. NPJ Parkinsons Dis. 8 (1), 170. https://doi.org/10.1038/s41531-022-00410-y.

Xue, J., Tao, K., Wang, W., & Wang, X. (2024). What Can Inflammation Tell Us about Therapeutic Strategies for Parkinson's Disease?. International journal of molecular sciences, 25(3), 1641. https://doi.org/10.3390/ijms25031641

Yamashita, K.Y., Bhoopatiraju, S., Silverglate, B.D., Grossberg, G.T., 2023. Biomarkers in Parkinson's disease: A state of the art review. Biomarkers in Neuropsychiatry. 9, 100074. https://doi.org/10.1016/j.bionps.2023.100074.

Yunna C., Mengru H., Lei W., Weidong C. (2020). Macrophage M1/M2 polarization. European journal of pharmacology, 877, 173090. https://doi.org/10.1016/j.ejphar.2020.173090

Zhao, Y., Huang, Y., Cao, Y., & Yang, J. (2024). Astrocyte-Mediated Neuroinflammation in Neurological Conditions. Biomolecules, 14(10), 1204. https://doi.org/10.3390/biom14101204

Zhu, F., Yue, W., & Wang, Y. (2014). The nuclear factor kappa B (NF-κB) activation is required for phagocytosis of staphylococcus aureus by RAW 264.7 cells. Experimental cell research, 327(2), 256–263. https://doi.org/10.1016/j.yexcr.2014.04.018